

# Periodicity and Atomic Ordering in Nanosized Particles of Crystals

Valeri Petkov,<sup>\*†</sup> Nick Bedford,<sup>†</sup> Marc R. Knecht,<sup>‡§</sup> Michael G. Weir,<sup>‡</sup> Richard M. Crooks,<sup>‡</sup> Wenjie Tang,<sup>‡</sup> Graeme Henkelman,<sup>‡</sup> and Anatoly Frenkel<sup>||</sup>

Department of Physics, 203 Dow Science, Central Michigan University, Mt. Pleasant, Michigan 48859, Department of Chemistry and Biochemistry, The University of Texas at Austin, 5300 Austin, Texas 78712, and Department of Physics, Yeshiva University, 245 Lexington Avenue, New York, New York 10016

Received: February 9, 2008; Revised Manuscript Received: March 19, 2008

Evidence is presented that nanosized particles of crystals do not necessarily adopt a periodic atomic structure as their bulk counterparts do and/or as predicted by theory. As an example, 1.6-nm Au particles grown inside a dendrimeric host are studied and found to possess a heavily disordered, metallic glass-type structure. The nanoparticle's structure evolves toward the face-centered-cubic-type lattice of bulk Au only upon removal of solvent. The results show that periodicity, which rules the structure and properties of bulk crystals, is less of a constraint at the nanoscale level and, therefore, may be used as tunable parameter in nanotechnology research.

## 1. Introduction

Atoms in bulk crystals are arranged in a periodic pattern over long-range distances and, hence, their properties are typically the sum of the equivalent contributions of a great number of identical units of atoms, known as unit cells. That is why the three-dimensional (3D) structure and properties of bulk crystals may be considered and explained well on the basis of periodic lattices built from such, usually fairly small, cells. With new technologies moving quickly toward smaller scales, nanosized particles of crystals are being produced in increasing numbers. The hope is that existing properties may be improved or emergent properties discovered when the size of the crystals approaches that of their unit cells. The new performance, however, does not come merely from the greatly enhanced surface-to-volume ratio of “nanocrystals”. In this paper, we present evidence that nanosized particles of crystals do not necessarily adopt a periodic 3D structure as their bulk counterparts do and/or as predicted by theory, and argue that this may affect their properties in a very substantial way. As an example, we consider 1.6 nm (~147 atom on average) Au particles grown inside a dendrimeric host. Bulk gold is exceptionally inert and naturally comes in crystals with a well-defined shape reflecting its face-centered-cubic-type (fcc) structure.<sup>1</sup> Nanosized particles of Au can, however, be catalytically<sup>2</sup> and optically<sup>3</sup> very active. The 147 Au atom particles we studied were tailored specifically for catalytic applications. Theory has predicted that Au particles of this so-called “magic” size should be well-ordered at the atomic scale and, just like bulk Au, might be viewed as stacks of regular atomic lattice planes. Accordingly, such particles are assumed to appear as highly symmetric bodies with a well-defined, faceted shape. Typical examples are truncated octahedra, decahedra, cubooctahedra, and so forth.<sup>4</sup> We find, however, that the atomic ordering in the nanoparticles we study may not be described in terms of periodic, lattice-

type structures. We make a point that this may be the case with many other nanosized particles of crystals and urge that this possibility is not overlooked in nanotechnology research.

## 2. Experimental Section

**2.1. Sample Preparation.** The Au nanoparticles were grown inside sixth-generation (G6) hydroxyl-terminated poly(amine) (PAMAM) dendrimers. Dendrimers are built from short polymeric branches radiating from a central core in a repetitive pattern. They appear globular in shape, and the G6 PAMAM dendrimer is about 6 nm in diameter. Higher-generation PAMAM dendrimers have dense peripheries, but their interiors are less dense and exhibit numerous nanosized cavities and channels that may provide storage space and diffusion pathways for small molecules and particles.<sup>5,6</sup> Au dendrimer-encapsulated nanoparticles (DENs) for EXAFS analysis are prepared employing the following procedure: to 237.0 mL of water, 5.00 mL of a 100 μM G6-OH solution was added with rigorous stirring. Next, 7.35 mL of a freshly prepared 10.0 mM aqueous solution of HAuCl<sub>4</sub> was added. This represents a metal:dendrimer ratio of 147:1. The solution was allowed to stir for <1 min, and then 10 equiv of NaBH<sub>4</sub> was added. The 1M NaBH<sub>4</sub> solution was freshly prepared in 0.30 M aqueous NaOH. The reduction reaction was allowed to proceed for 1.0 h prior to analysis. Solid (i.e., dry) samples were prepared by lyophilization (Freezone 12, Labconco Corp.). For XRD analysis, Au DENs were prepared identically, except the total volume of the solution was reduced from 250.00 to 10.00 mL. Thus obtained Au DENs are denoted hereafter as G6-Au<sub>147</sub>.

**2.2. Morphology and Structure Characterization.** The size and shape of the nanoparticles were studied by transmission electron microscopy. Figure 1 shows a TEM image of a collection of dry G6-Au<sub>147</sub> DENs, a size distribution extracted from it, and a HRTEM of a single DEN.

The local atomic structure of the nanoparticles was studied by extended X-ray absorption fine-structure (EXAFS) spectroscopy.<sup>7</sup> EXAFS experiments were carried out at beamline X18B at the National Synchrotron Light Source (NSLS). Both dry and wet (i.e., kept in aqueous solution) G6-Au<sub>147</sub> particles were measured at the Au L3 edge (11,919 eV) from 150 eV below

\* Corresponding author. E-mail: petkov@phy.cmich.edu.

† Central Michigan University.

‡ The University of Texas at Austin.

§ Current address: University of Kentucky, 101 Chemistry-Physics Building, Lexington, Kentucky 40506.

|| Yeshiva University.

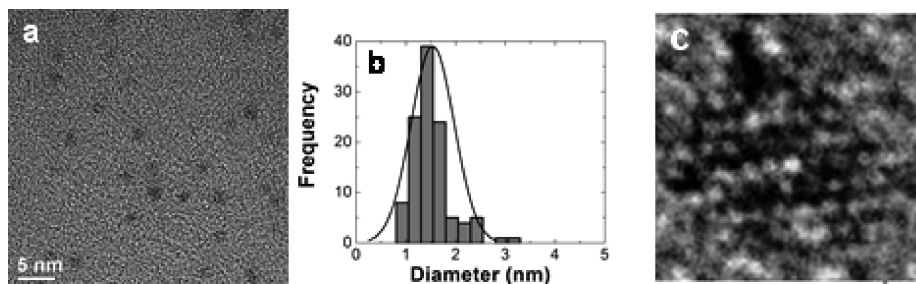


**Figure 1.** TEM images of dry Au DENs (a) and the corresponding size distribution (b). High-resolution TEM of one the largest DENs is shown in part c.

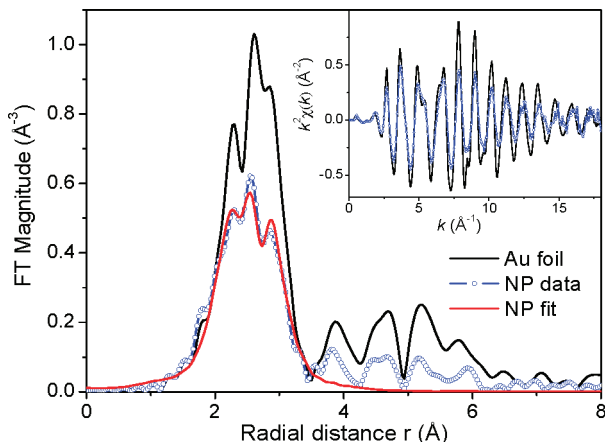


**Figure 2.** Fourier-transformed,  $k^2$ -weighted EXAFS data and the best fit for dry G6- $\text{Au}_{147}$  in  $r$ -space, uncorrected for the photoelectron space shift. Comparison with Au foil data is shown in  $r$ -space and  $k$ -space (inset).

to 1530 eV above it. Data analysis was carried out using the IFEFFIT and FEFF6 software packages as described previously.<sup>8</sup> Real-space spectra of the data and best fit of FEFF6 theory are shown in Figure 2.

The 3D atomic ordering in both dry and wet nanoparticles was probed by total XRD and atomic pair distribution function (PDF) analysis. The experiments were carried out at the beamline 11IDB at the Advanced Photon Source, Argonne National Laboratory using X-rays of energy 90.48 keV ( $8 = 0.137 \text{ \AA}$ ) and a large area (General Electric) detector. Synchrotron radiation X-rays were used for two reasons. First, the higher flux of synchrotron radiation X-rays makes it possible to measure the rather weak diffraction patterns of G6- $\text{Au}_{147}$  particles with very good statistical accuracy. Second, the higher energy of synchrotron radiation X-rays makes it possible to reach higher wave vectors,  $Q$ . Both are important prerequisites for the success of the PDF analyses employed here.<sup>10</sup>

### 3. Results and Discussion

As can be seen in Figure 1a, Au DENs are spherical in shape and, as intended, show a very narrow size distribution centered at about 1.6(3) nm (Figure 1b). However, high-resolution images of individual particles do not exhibit well-defined, lattice-type fringes and a faceted morphology (see Figure 1c) as is typically observed for crystalline Au.

The EXAFS results for the average Au–Au first neighbor coordination number (CN) and distance in dry G6- $\text{Au}_{147}$  particles are  $N_1 = 9.0(9)$  and  $r_1 = 2.832(6) \text{ \AA}$ , respectively. In wet G6- $\text{Au}_{147}$ , those numbers are  $N_1 = 8.9(7)$  and  $r_1 = 2.836(4)$ , respectively. The CN is consistent with the theoretical  $N_1$  of 8.98 for a 147-atom cuboctahedron and 9.09 for a 140-atom

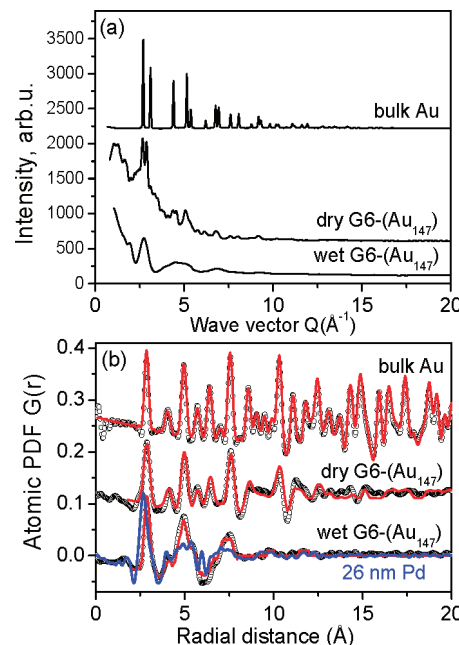


**Figure 3.** Experimental XRD (a) and the corresponding PDFs  $G(r)$  for 1.6-nm Au particles (b). Best model PDFs (line in red) and an experimental PDF for 26-nm Pd particles (line in blue) are shown as well.

truncated octahedron. Both are stacks of atomic planes occurring with the fcc-type lattice but have different shapes.<sup>4</sup> Clearly, it is difficult to discriminate between these two, and other, competitive 3D models using the EXAFS data alone. The metallic character of G6- $\text{Au}_{147}$  is evident from comparing the EXAFS data for the nanoparticles and bulk Au (Figure 2). The fact that  $r_1$  in the nanoparticles is shorter than that in the bulk ( $2.87 \text{ \AA}$ ) can be attributed to an enhanced surface tension.<sup>9</sup> No detectable Au bonding to ligands was observed by EXAFS at distances below the first Au–Au peak, indicating that the surface of the G6- $\text{Au}_{147}$  particles is, at most, only partially passivated by the dendrimer host. In particular, incorporation of Au–N/O bonds with a realistic mean square disorder,  $\sigma^2 = 0.005 \text{ \AA}^2$ , into the structural model used in the EXAFS data analysis results in a very small (0.1) upper limit of Au–N/O CN. For a 1.6(3)-nm particle, this would correspond to a total number of about 15 Au–O/N bonds, indicating that at least 84% of metal atoms at the G6- $\text{Au}_{147}$  surface are free to participate in catalytic reactions.

Experimental XRD patterns for wet (i.e.,  $2.00 \mu\text{M}$  aqueous solution) of G6- $\text{Au}_{147}$  particles and dry G6- $\text{Au}_{147}$  particles are shown in Figure 3. Bulk Au (crystalline grains several hundred nanometers in size) was also measured and used as a standard. Sharp Bragg peaks are present in the XRD pattern for bulk Au (Figure 3a). Obviously, the material is well-ordered at the atomic

scale and, hence, acts as an almost perfect diffraction grating when irradiated with X-rays. Alternatively, the XRD patterns for both dry and wet G6-Au<sub>147</sub> particles are rather diffuse as is often observed with materials whose structure lacks periodic atomic order such as glasses and liquids. Such diffraction patterns are virtually impossible to analyze by traditional approaches that rely on sharp Bragg peaks such as Rietveld analysis.<sup>11</sup> However, as demonstrated recently,<sup>12</sup> when reduced to the corresponding atomic PDF the same experimental XRD data lend themselves to structure search and refinement. The experimental PDFs  $G(r) = 4\pi r[\rho(r) - \rho_0]$ , where  $\rho(r)$  and  $\rho_0$  are the local and average atomic number density, respectively, for all samples measured are shown in Figure 3b. The raw XRD data reduction and PDF derivation was done with the help of the program RAD.<sup>13</sup> As can be seen in the top part of Figure 3b,  $G(r)$  for bulk Au exhibits a series of well-defined peaks to high real-space distances each reflecting a particular, well-defined coordination sphere. The experimental data can be approximated very well in terms of a structure model based on a periodic (fcc)-type lattice (S.G.  $Fm\bar{3}m$ ) with a four-atom unit cell, 4.07 Å in length. Model calculations were done using the program PDFFIT.<sup>14</sup> The first peak in the experimental PDFs for both dry and wet Au nanoparticles is positioned at 2.87(2) Å, consistent with the first neighbor distance in bulk Au, confirming the metallic character (i.e., the zero valence state) of G6-Au<sub>147</sub>. In agreement with the EXAFS data, the experimental PDFs do not show physically sensible peaks at shorter distances, which means there is no indication of the presence of a substantial number of bonds between the dendrimer and Au<sub>147</sub> particle surface. The higher- $r$  peaks in the PDFs for nanoparticles line up with those in the PDF for bulk Au, indicating that the atomic ordering in the nanoparticles bears some similarities to that in a fcc-type structure. However, the peaks in the PDFs for both the wet and dry G6-Au<sub>147</sub> particles are very broad and decay to zero at distances as short as 10 and 15 Å, respectively. Clearly the sequence of coordination spheres in the nanoparticles is neither as well-defined nor so extended as it would be in a nanosized stack of well-defined atomic planes.<sup>15</sup> The observed structural disorder may not be neglected because it rendered unsuccessful all attempts to approximate the experimental PDF data for Au<sub>147</sub> DENs with models based on periodic structures, including a fcc-type lattice. In other words, it was not possible to find a characteristic unit cell or set(s) of atomic planes that, when stacked in a periodic manner, would approximate the experimental PDFs at an acceptable confidence level. Because of their high degree of periodicity, all such models show atomic PDFs composed of several well-defined peaks that are not seen in the experimental data. Alternatively, structurally disordered, nonperiodic models generated by reverse Monte Carlo (RMC) simulations did a very good job in approximating all details in the experimental data, as the results presented in Figure 3b show. Such a high level of agreement is a must so that nanoparticle's properties are considered in terms of a proper structure model.

A great advantage of the RMC simulation technique is that it relies entirely on available experimental information.<sup>16a</sup> The technique involves placing atoms in a simulation box and moving them around so that the difference between the model computed and experimental structure-sensitive quantities, the experimental PDF data in our case, become as small as possible. Models for G6-Au<sub>147</sub> particles were made spherical in shape, mimicking the nanoparticle's shape revealed by TEM (see Figure 1). Additionally, the simulations were carried out keeping an ample empty space between the model atomic configuration

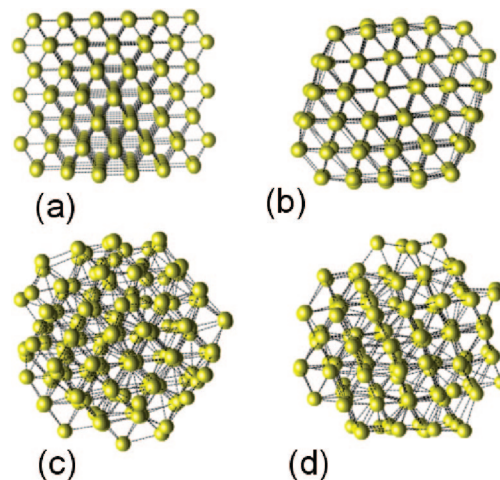


**Figure 4.** Fragment (147 atom) of the fcc lattice of bulk Au (a), 140-atom truncated octahedron as generated by DFT alone, (b) and RMC generated models of wet (c) and dry (d) G6-Au<sub>147</sub> particles.

and the simulation box walls, mimicking the free nanoparticle surface. Furthermore, while being moved around, atoms were required to pack as closely to each other as possible, thus emulating the metallic character of Au–Au interatomic interactions. Unless this constraint was imposed, the resulted model configurations had free surfaces that are too rough and exhibited an average Au–Au first CN lower than that found by EXAFS. Initial configurations with various degrees of periodicity, ranging from a random dense packing of atoms to a fcc-type lattice, and with sizes of 147 (+/−30) atoms, exhibited by at least 85% of the particles (see the size distribution in Figure 1b), were explored. Under the described simulation conditions, none have been found to bias the essential characteristics of the final structure solutions found. All calculations were done with the program RMC++.<sup>16b</sup>

A disadvantage of the RMC simulation technique, which may be managed easily as shown here, is that the structural models it generates are the most disordered (i.e., with the highest configurational entropy/energy possible) ones that agree with the available experimental information. That is why the RMC generated models were relaxed further by minimizing their total energy, calculated with density functional theory (DFT). The DFT calculations used the PW91 functional,<sup>17</sup> a plane wave basis set with a 250 eV cutoff and pseudopotentials within the projector augmented wave framework<sup>18</sup> as implemented in the VASP code.<sup>19</sup> After minimization, a 1-ps molecular dynamics calculation at a temperature of 500 K was used to ensure that the system was not trapped in a shallow local minimum. The energy of the models dropped substantially when relaxed. For example, the energy of a 147-atom model of wet G6-Au<sub>147</sub> particles dropped from −2.54 to −2.82 eV/Au, but the model topology changed very little. For reference, the binding energy of a 140-atom truncated octahedron is −2.86 eV/Au and that for bulk Au is −3.05 eV/Au. Exemplary structure models for wet (RMC generated and DFT relaxed) and dry (RMC generated) G6-Au<sub>147</sub> particles are shown in Figure 4. A 147-atom fragment of the fcc lattice of bulk gold, and a truncated octahedron of 140 atoms resulted from DFT model calculations alone are shown in Figure 4 as well. Note, when not based on RMC generated initial configuration, that is, on experimental structure-sensitive data, DFT theory predicts model structures that are very well-ordered internally, periodic and, hence, with a regular shape. As can be seen in Figure 4, the RMC/experimental-data-based model structures show signatures of

local fcc-type ordering but are essentially nonperiodic and not quite regular in shape. Such a type of 3D structure is usually seen with bulk metallic glasses.<sup>20</sup> Here it is to be noted that the atomic ordering periodicity may be broken not only with 1–2 nm Au DENs where a very large fraction (50 to 30%) of the atoms are at or very close to the particle's surface. We have found that 26-nm particles of Pd, that, like Au, is always an fcc-type crystal while in bulk, also exhibit an atomic PDF (see Figure 3b) that may be explained only in terms of a heavily disordered, nonperiodic structure.<sup>12a</sup> Similar behavior has been observed with nonmetallic nanosized particles (e.g., semiconductor quantum dots)<sup>21</sup> as well.

The lack of periodicity in the 3D structure of nanosized particles may have an important implication on their properties. In particular, the nanoparticles may not necessarily come in a well-defined, faceted shape (see Figure 4c and d) as crystalline (Figure 4a) or related ordered structures (Figure 4b) of a comparable size would do. In other words, the nanoparticles' surface may not be made of a family of regular atomic lattice planes, but rather it might be somewhat curved and/or less densely packed as, for example, recent high-resolution STEM images show (see Figure 3 in ref 22). Also, as shown recently,<sup>23</sup> the electronic/band structure and, hence, the way the nanoparticle surface and adsorbates interact, may be quite different for nanoparticles with periodic and nonperiodic 3D structures. This may render structurally disordered particles with a curved surface catalytically more (or less) active than nanosized particles with periodic 3D structures and faceted shapes. Optical, magnetic, and transport properties are also known to be highly dependent on the atomic-scale structure type. Obviously, those may also be affected substantially when it is nonperiodic. When the latter occurs, the nanoparticles' properties may not be the sum of equivalent contributions of identical building units arranged in good accord. Rather, they may appear as an intricate convolution of contributions coming from somewhat similar but structurally incoherent nanoparticle fractions instead.

#### 4. Conclusions

In conclusion, PAMAM dendrimers may be used as templates for producing almost monodisperse metallic particles with a size of up to 2 nm in a controlled way. The particles sit in the dendrimer cavities as illustrated in Figure 5 but are free to participate in catalytic reactions. Because the nanoparticles likely form through a diffusion controlled by a polymeric host and self-assembly mechanism and/or are topologically constrained inside the polymeric matrix, they do not appear with a fcc or other lattice-type structure. Instead, they are a nonperiodic, dense packing of Au atoms that shows some signatures of the fcc-type structure only. That packing is indeed quite stable: compare  $-2.82 \text{ eV/Au}$  versus  $-2.86 \text{ eV/Au}$  for the periodic and nonperiodic structures shown in Figure 4b and c, respectively. It is, however, possible to be modified by extra processing. For example, the crystallinity of Au DENs clearly increases when they are dried in air (see Figures 3 and Figure 4) or when alternative technological routes are employed.<sup>15</sup> Obviously, depending on the technological route and/or the postpreparation treatment, different batches of nanosized particles of crystals may adopt either periodic or nonperiodic type 3D structure and, hence, exhibit *different properties* even when their *size and surface area* are essentially the same.

Another message of our work is that the 3D structure of nanosized particles of crystals should not automatically be assumed to be periodic. Our present and previous studies show that the periodicity of atomic ordering may be partially or fully

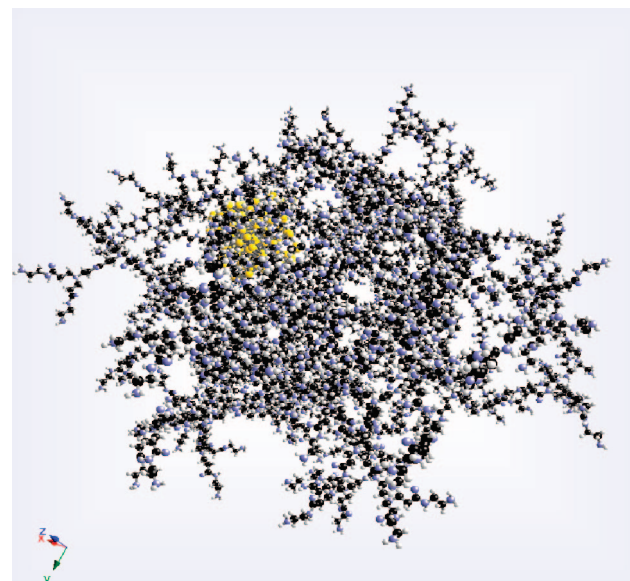


**Figure 5.**  $\text{Au}_{147}$  atom particle (yellow) inside one of the cavities of a G6 PAMAM dendrimer. The particle is the one shown in Figure 4c,<sup>6</sup> the PAMAM 3D structure was determined in a previous study.<sup>6</sup>

broken with 1.6 nm to at least 26 nm particles of various crystalline materials, metallic and nonmetallic. Periodicity thus appears not to be much of a constraint on the 3D structure and, hence, properties of nanosized particles of crystals, as it is for bulk crystals, and, therefore, may be used as an extra tunable parameter in nanotechnology research. This opportunity is being recognized<sup>24,25</sup> but yet remains largely unutilized. We believe our work will encourage researchers to exploit it to a larger extent. The success of the effort along this line would require a very precise determination of the atomic ordering inside nanosized particles so that their properties are considered in terms of the right structure type, be it periodic or not.<sup>26</sup> As demonstrated here, a set of experimental and computational techniques is already available to tackle this challenging task<sup>27</sup> with success.

**Acknowledgment.** Financial support of this project was provided by the DoE-BES Grants DE-FG02-03ER15468 (RMC) and DE-FG02-03ER15476 (AIF). Work at the NSLS was supported by DoE Grants DE-FG02-03ER15688 and DE-AC02-98CH10886 while at the APS by DoE contract W-31-109-ENG-38. V.P. acknowledges support from CMU through Grant REF 60628 and the help of Peter Chupas, APS, with the high-energy XRD measurements. M.K. and M.W. acknowledge the assistance of Nebojsa Marinkovich for assistance with the EXAFS experiments. We acknowledge the Robert A. Welch Foundation and SPRING for support of some of the facilities used to carry out this project.

#### References and Notes

- (1) McKeehan, L. W. *Phys. Rev.* **1922**, *20*, 424.
- (2) Chen, M. M.; Goodman, D. W. *Acc. Chem. Res.* **2006**, *39*, 739.
- (3) Daniel, M.-C.; Astruc, D. *Chem. Rev.* **2004**, *104*, 293.
- (4) Doye, J. P. K.; Wales, D. J. *J. Chem. Phys. Lett.* **1995**, *247*, 339.
- (5) Scott, R. W. J.; Wilson, O. M.; Crooks, R. M. *J. Phys. Chem.* **2005**, *109*, 692.
- (6) Petkov, V.; et al. *Solid State. Commun.* **2005**, *134*, 671.
- (7) (a) Lytle, F. W.; Via, G. H.; Sinfelt, J. H. *J. Chem. Phys.* **1977**, *67*, 3831. (b) Frenkel, A. I.; Hills, C. W.; Nuzzo, R. G. *J. Phys. Chem. B* **2001**, *105*, 12689.
- (8) Frenkel, A. I.; et al. *J. Chem. Phys.* **2005**, *123*, 184701.
- (9) Mays, C. W.; Vermaak, J. S.; Kuhlmann-Wilsdorf, D. *Surf. Sci.* **1968**, *12*, 134.

- (10) Egami, T.; Billinge, S. J. L. In *Underneath the Bragg Peaks*; Pergamon Press: Amsterdam, 2003.
- (11) Rietveld, H. M. *J. Appl. Crystallogr.* **1968**, *2*, 65.
- (12) (a) Petkov, V.; Ohta, T.; Hou, Y.; Ren, Y. *J. Phys. Chem. C* **2007**, *111*, 714. (b) Petkov, V.; et al. *Phys. Rev B* **2005**, *69*, 085410.
- (13) Petkov, V. *J. Appl. Crystallogr.* **1989**, *22*, 387.
- (14) Proffen, Th.; Billinge, S. J. L. *J. Appl. Crystallogr.* **1999**, *32*, 572.
- (15) Petkov, V.; Peng, Y.; Williams, G.; Huang, B.; Tomalia, D.; Ren, Y. *Phys. Rev. B* **2005**, *72*, 95402.
- (16) (a) McGreevy, R. L.; Pusztai, L. *Mol. Sim.* **1988**, *1*, 359. (b) Evrard, G.; et al. *J. Phys.: Condens. Matter* **2005**, *17*, S1.
- (17) Perdew, J. P.; Wang, Y. *Phys. Rev. B* **1992**, *45*, 13244.
- (18) Blochl, P. E. *Phys. Rev. B* **1994**, *50*, 17953.
- (19) Kresse, G.; Furthmüller, J. *Comput. Mater. Sci.* **1996**, *6*, 15.
- (20) Lamparter, P. *Phys. Scr.* **1995**, *T57*, 45.
- (21) Pradhan, S. K.; Deng, Z. T.; Tang, F.; Wang, C.; Ren, Y.; Moeck, P.; Petkov, V. *J. Appl. Phys.* **2007**, *102*, 044304.
- (22) Li, Z. Y.; et al. *Nature* **2008**, *451*, 46.
- (23) Sun, Y.; Zhuang, L.; Xinlin, J. L.; Liu, P. *J. Am. Chem. Soc.* **2007**, *129*, 15465.
- (24) Huang, W.; Qian, W.; El-Sayed, M. A.; Ding, Y.; Wang, Zh. *Phys. Chem. C* **2007**, *111*, 10751.
- (25) Tang, Y.; Ouyang, M. *Nat. Mater.* **2007**, *6*, 754.
- (26) In contrast to periodic/lattice-type models (e.g., four-atom unit cell of an fcc lattice) nonperiodic ones usually have a much larger number of parameters (e.g., the coordinates of all 147 atoms in the model configuration of a 1.6-nm Au particle). Given the recent progress in computer power, this becomes less and less of an obstacle in structure–property prediction studies.
- (27) Billinge, S. J. L.; Levin, I. *Science* **2007**, *316*, 561.

JP801195C